

Precise Stark-effect investigations of the lithium D_1 and D_2 lines

L. Windholz, M. Musso, G. Zerza, and H. Jäger

Institut für Experimentalphysik, Technische Universität Graz, Petersgasse 16, A-8010 Graz, Austria

(Received 16 January 1992; revised manuscript received 21 May 1992)

The Stark shift and splitting of the resonance lines of the lithium atom were investigated in electric fields up to 420 kV/cm, using laser-atomic-beam spectroscopy. The scalar and tensor polarizabilities of the levels $2^2P_{1/2}$ and $2^2P_{3/2}$ of both isotopes ^7Li and ^6Li were accurately determined. The experimentally obtained level polarizabilities are compared with theoretically calculated values.

PACS number(s): 32.60.+i

I. INTRODUCTION

Shortly after the discovery of the influence of an external electric field on atomic spectral lines by Stark in 1913, several authors have published Stark-effect investigations on the sodium resonance lines (a survey is given in the paper of Windholz and Musso [1]). However, up to 1957, practically no publications can be found concerning Stark-effect experiments on the lithium resonance lines. In that year Blamont [2] reported on optical double-resonance studies of the Stark effect of Li I lines. Budick, Marcus, and Novick [3] in 1965 dealt with the Stark shift of the 3^2P levels of ^7Li using level-crossing spectroscopy. Molof *et al.* [4] reported in 1974 values of the ground-state polarizabilities of alkali-metal and noble-gas atoms, using the magnetic-field-electric-field-gradient balance technique.

Apart from these measurements, no experimental values of the Stark-shift parameters of the Li D_1 and D_2 lines could be found until very recently. In our opinion, this has two reasons: (i) The wavelength (671 nm) is not well suited for visual observations or for photographic plates when performing interference spectroscopy. (ii) The Stark shifts of the lithium D lines are about five times smaller than those of sodium; so one needs very high field strengths to produce observable line shifts. Nevertheless, many theoretical works have been published since the Stark effect of the alkali-metal atoms is of general physical interest. For this reason, we tried to use our experience in producing high electric field strengths in order to obtain accurate Stark-shift measurements of these lines; preliminary results were presented in Ref. [5]. Very recently Hunter *et al.* [6] published very accurate values of the Stark shift of the D_1 line of lithium for field strengths up to 35 kV/cm.

II. EXPERIMENT

A properly collimated atomic beam is crossed perpendicularly by the exciting laser beam in the field arrangement shown in Fig. 1. This arrangement is well suited for field strengths up to about 500 kV/cm but does not allow an accurate determination of the field strength itself. [The accuracy is limited by the mechanical measurement of the field-plate spacing (≈ 0.4 mm) to approximately

2%.] Therefore, for highly accurate measurements up to 100 kV/cm we used another field arrangement in which the metallic layers on the plates of a Fabry-Pérot interferometer are connected to a high-voltage source in order to produce an electric field between the plates. The spacing of this actively stabilized interferometer was determined with high accuracy [0.5656(1) mm] from a measurement of its free spectral range by means of a tunable dye laser and a wave meter. Further information about this method can be found in Refs. [1,7-11]. Together with an accurate measurement of the applied voltage this leads to an accurate value for the electric-field strength. By comparing the shifts obtained with each field arrangement it was possible to calibrate accurately the high-field arrangement (field uncertainty 0.13%) against the Fabry-Pérot field arrangement (uncertainty 0.03%). The shifts of the line components were measured in the usual way against frequency marks generated by a confocal Fabry-Pérot étalon with a free spectral range of 197.5974(3) MHz (see Ref. [12]).

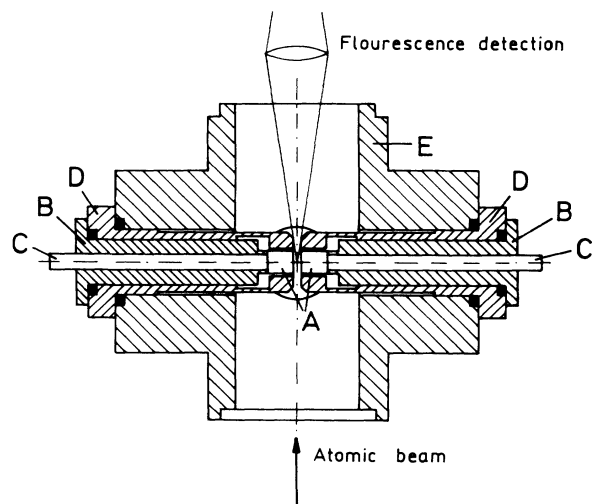


FIG. 1. High-field arrangement. A, stainless-steel field plates; B, glass ceramics insulator; C, field voltage connections; D, field shielding (stainless steel); E, ground body (aluminum).

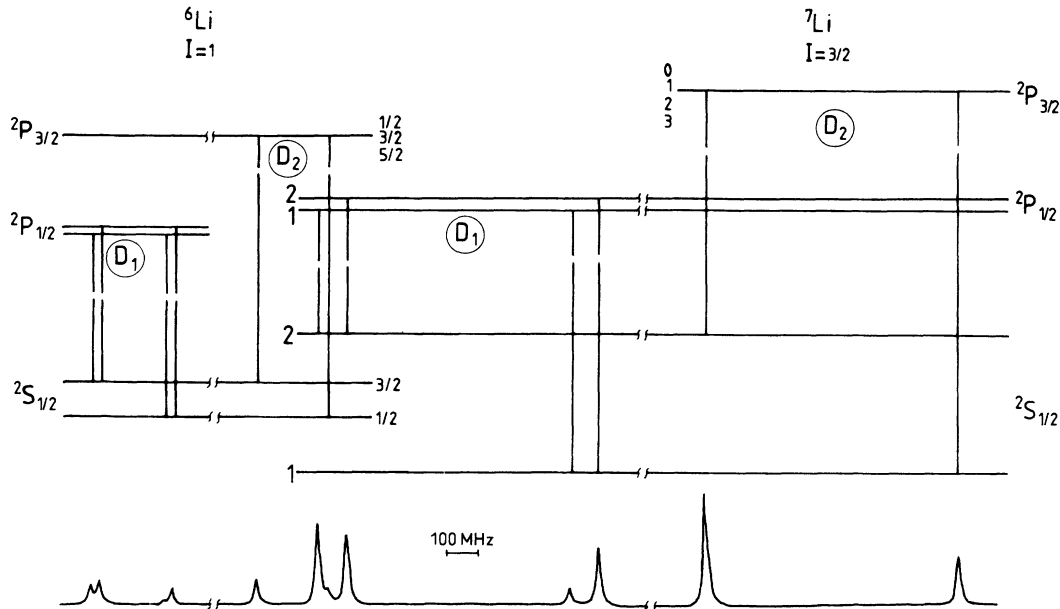


FIG. 2. Zero-field hyperfine spectrum of ${}^6\text{Li}$ and ${}^7\text{Li}$. The hyperfine splittings of $2^2P_{3/2}$ levels are not resolved. The isotopic shifts are 10 534.3(3) MHz for the D_1 lines and 10 539.9(12) MHz for the D_2 lines, respectively; the fine-structure splitting of the 2P levels was determined to be 10 050.2(15) MHz for ${}^6\text{Li}$ and 10 056.6(15) MHz for ${}^7\text{Li}$, respectively [12].

III. OBSERVED SPECTRA

The zero-field hyperfine spectrum of the lithium resonance lines consists of three groups of components. As shown in Fig. 2, we observe from left to right the hyperfine components of ${}^6\text{Li } D_1$, then ${}^6\text{Li } D_2$ partly overlaid by the more intense components of ${}^7\text{Li } D_1$, and then the components of ${}^7\text{Li } D_2$. The intensities of ${}^6\text{Li}$ and ${}^7\text{Li}$ are related to the natural abundances (7.4% and 92.6%, respectively). The fine-structure splitting is about 10 GHz and has nearly the same value as the isotopic line shift. The hyperfine splitting of $2^2P_{3/2}$ is not resolved (hyperfine constants of ${}^7\text{Li } 2^2P_{3/2}$: $A \approx -3$ MHz, $B \approx -0.2$ MHz) in the field-free spectra. Nevertheless, from spectra in magnetic fields [12] we were able to determine all involved hyperfine constants (except those of ${}^6\text{Li } 2^2P_{3/2}$), the isotopic shift, and the fine-structure splitting.

In Figs. 3(a)–3(d) the behavior of two line groups in high electric fields is shown.

IV. EVALUATION OF THE SPECTRA

As mentioned before the field strength must be known with very high accuracy in order to be able to deduce with high accuracy polarizabilities from the line shifts and splittings. From the optical measurement of the free spectral range of the Fabry-Pérot field arrangement [9] together with a proper field voltage measurement we were able to determine electric-field strengths (up to 100 kV/cm) with relative errors below 3×10^{-4} . In order to evaluate a good value of the scalar polarizabilities, we recorded each component group at fixed field strength of approximately 100 kV/cm several times, separately for

excitation with σ - and π -polarized laser light. At these field strengths, no splitting of the D_2 lines is observable. Thus, we were able to determine only the scalar polarizabilities.

For evaluating the tensor polarizabilities, which are responsible for the splitting of the D_2 lines [as can be seen in Figs. 3(a) (${}^6\text{Li}$) and 3(c) (${}^7\text{Li}$)], we were forced to use the spectra taken with the high-field arrangement. With the help of the now known scalar polarizabilities, we calibrated the high-field arrangement by the line shift for a given field voltage. In this way the field strength was more accurately determined than from the previous rough mechanical measurement of the spacing. From the splitting in high fields we derived the tensor polarizabilities of the $2^2P_{3/2}$ levels.

For a very accurate determination of the polarizabilities, the (unresolved) hyperfine structure of $2^2P_{3/2}$ should be considered additionally. We were able to calculate the Stark splitting of this level using the same procedures as mentioned in Ref. [1] in order to take into account slight changes in the positions and intensities of the hyperfine line components. In this way we could fit theoretical line positions to the experimental ones handling the scalar and tensor polarizabilities as free parameters.

V. THEORY

The interaction between the atom and a uniform electric field is described by the Hamiltonian operator

$$H_E = -\mathbf{E} \cdot \mathbf{p}, \quad (1)$$

where \mathbf{E} is the electric field and $\mathbf{p} = -e\mathbf{r}$ is the electric dipole moment operator. Since \mathbf{r} has nonzero matrix ele-

ments only between states of opposite parity, the mean value of H_E in all eigenstates vanishes, independently from their parity. Hence the change in energy of a state $|a\rangle$ is given by the second-order perturbation formula

$$\Delta E(a) = \sum_b \frac{\langle a | H_E | b \rangle \langle b | H_E | a \rangle}{E_a - E_b} = \langle a | H'_E | a \rangle, \quad (2)$$

where the sum extends over all intermediate states $|b\rangle$ of the atom. Using the effective Hamiltonian H'_E , the Stark shift formally is equivalent to a first-order perturbation.

Following the formalism given by Angel and Sandars [13] and taking the electric field direction as the z axis, the interaction Hamiltonian H'_E is given by

$$H'_E = -\frac{1}{2} \left\{ \alpha_0 + \alpha_2 \frac{3J_z^2 - J(J+1)}{J(2J-1)} \right\} E^2, \quad (3)$$

with the scalar polarizability α_0 and the tensor polarizability α_2 (J is the total angular-momentum quantum number, J_z the projection of the operator J in the direction z). Neglecting the hyperfine structure the frequency shift of a level ν_i can be expressed as

$$\Delta \nu_i = -\frac{1}{2} \left\{ \alpha_{0,i} + \alpha_{2,i} \frac{3M_J^2 - J(J+1)}{J(2J-1)} \right\} E^2, \quad (4)$$

where M_J is the projection quantum number of J .

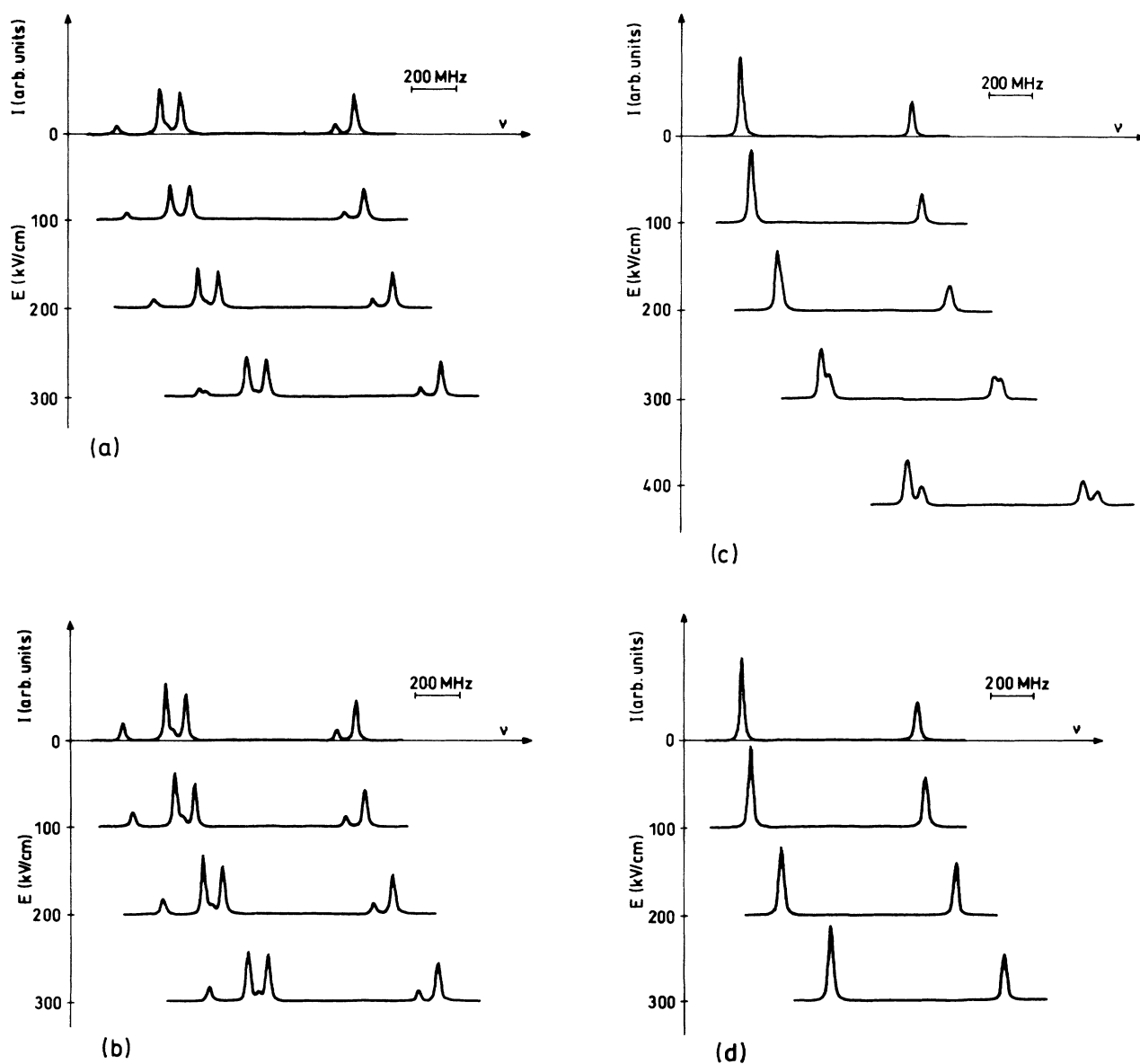


FIG. 3. Examples of high-field Stark spectra. (a) ${}^6\text{Li } D_2 + {}^7\text{Li } D_1$, exciting laser light is σ -polarized; (b) ${}^6\text{Li } D_2 + {}^7\text{Li } D_1$, exciting laser light π -polarized; (c) ${}^7\text{Li } D_2$, exciting laser light σ -polarized; (d) ${}^7\text{Li } D_2$, exciting laser light π -polarized.

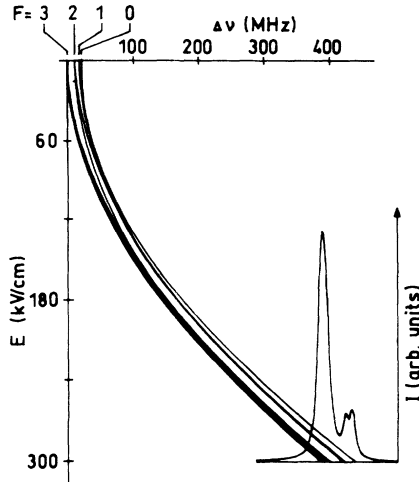


FIG. 4. Calculated Stark splitting of the transition pattern ${}^7\text{Li } 2^2S_{1/2}, F=2$ to $2^2P_{3/2}, F=3, 2, 1, 0$ in electric fields up to 300 kV/cm. For 300 kV/cm, the theoretical line profile is shown (exciting laser light is σ -polarized).

For an accurate determination of the polarizabilities from the observed spectra the hyperfine structure of the levels involved has to be taken into account. The Stark shifts and splittings for an atom with hyperfine structure are obtained by diagonalization of the Hamiltonian

$$H = H'_E + H_{\text{hfs}}, \quad (5)$$

where the hyperfine interaction is expressed in terms of the magnetic dipole and electric quadrupole coupling constants A and B ,

$$H_{\text{hfs}} = hA \mathbf{I} \cdot \mathbf{J} + hB \frac{3(\mathbf{I} \cdot \mathbf{J})^2 + 3\mathbf{I} \cdot \mathbf{J} - I(I+1)J(J+1)}{2I(I-1)J(2J-1)}. \quad (6)$$

From the shift and splitting of the levels involved in the transition the shift and splitting of the line components can be calculated. The programs used for these calculations are described elsewhere in more detail [14].

A simulation of the hyperfine pattern in fields up to 300 kV/cm is shown in Fig. 4 (transition $2^2S_{1/2}, F=2$ to $2^2P_{3/2}, F=3, 2, 1, 0$). Performing the simulation, our experimental values of the polarizabilities were used. The line profiles are drawn with the calculated intensities choosing a Lorentzian line profile with a full width at half maximum (FWHM) close to the experimentally observed value (15 MHz). The slight changes in the centers of the components due to the hyperfine-structure Stark effect were taken into account in the data evaluation of our experiment.

The general behavior of the D_1 and D_2 lines is a shift given — following Eq. (4) — by

$$\Delta\nu_{\text{line}} = k_{\text{line}} E^2.$$

In the case of the D_1 line we obtain the Stark-shift parameter $k_{D_1} = -\frac{1}{2}(\alpha_{0,2P_{1/2}} - \alpha_{0,2S_{1/2}})$ which is valid also for each of the four hyperfine components.

In the case of the D_2 line the presence of α_2 causes a splitting of the line into two groups, one with $|M_J| = \frac{1}{2}$ and the other with $|M_J| = \frac{3}{2}$, therefore

$$k_{D_2, |M_J|=1/2} = -\frac{1}{2}(\alpha_{0,2P_{3/2}} - \alpha_{0,2S_{1/2}} - \alpha_{2,2P_{3/2}})$$

and

$$k_{D_2, |M_J|=3/2} = -\frac{1}{2}(\alpha_{0,2P_{3/2}} - \alpha_{0,2S_{1/2}} + \alpha_{2,2P_{3/2}}).$$

However, the last two relations are exactly valid only for Stark splittings much larger than the hyperfine splitting as can be seen in Fig. 4.

VI. POLARIZABILITIES

The results obtained after fitting the theoretical line positions to the experimental ones handling the scalar and tensor polarizabilities of the first excited state as free parameters are given in Table I. For the ground-state polarizability we used the experimental value obtained by Molof *et al.* [4]. Table II presents the Stark-shift parameters k_{line} obtained from the level polarizabilities of Table I.

Calculations of α_0 and α_2 for $2^2P_{3/2}$ were performed,

TABLE I. Experimentally determined values of the scalar polarizability α_0 and the tensor polarizability α_2 [in kHz/(kV/cm)²] of the levels involved. In the data evaluation the value $\alpha_0 = 40.8$ kHz/(kV/cm)² of Molof *et al.* [4] was used. The errors (90% confidence level) are given relative to this value of $\alpha_{0,2S_{1/2}}$ (assumed to be exact in our data evaluation).

Isotope	Level	α_0	α_2	Reference
${}^7\text{Li}$	$2^2S_{1/2}$	40.8(8)		[4]
${}^6\text{Li}$	$2^2P_{1/2}$	31.56(15)		This work
${}^6\text{Li}$	$2^2P_{3/2}$	31.63(17)	+0.406(11)	This work
${}^7\text{Li}$	$2^2P_{1/2}$	31.57(8)		This work
${}^7\text{Li}$	$2^2P_{3/2}$	31.52(9)	+0.409(11)	This work
${}^6,7\text{Li}$	$2^2P_{1/2}$	31.557(2)		[6]

TABLE II. Stark-shift parameters ($\Delta\nu = k_{\text{line}} E^2$) [k in kHz/(kV/cm²)].

Isotope	Line	k_{line}	Reference
⁶ Li	D_1	4.6220(25)	[6]
	D_1	4.618(76)	This work
	D_2 $ M_J = \frac{1}{2}$	4.786(88)	This work
	D_2 $ M_J = \frac{3}{2}$	4.380(88)	This work
⁷ Li	D_1	4.6212(25)	[6]
	D_1	4.617(41)	This work
	D_2 $ M_J = \frac{1}{2}$	4.845(52)	This work
	D_2 $ M_J = \frac{3}{2}$	4.436(52)	This work

e.g., by Schmieder, Lurio, and Happer [15]. The polarizabilities can be expressed as

$$\alpha_0 = -[9D_{(5/2)} + D_{(3/2)} + 10S_{(1/2)}]/45, \quad (7)$$

$$\alpha_2 = [9D_{(5/2)} - 4D_{(3/2)} + 50S_{(1/2)}]/225, \quad (8)$$

with

$$S_{(1/2)} = \sum_{n'} \frac{|\langle 2P || p || n'S \rangle|^2}{W(2P_{3/2}) - W(n'S_{1/2})}, \quad (9)$$

$$D_{(3/2)} = \sum_{n'} \frac{|\langle 2P || p || n'D \rangle|^2}{W(2P_{3/2}) - W(n'D_{3/2})}, \quad (10)$$

$$D_{(5/2)} = \sum_{n'} \frac{|\langle 2P || p || n'D \rangle|^2}{W(2P_{3/2}) - W(n'D_{5/2})}, \quad (11)$$

TABLE III. Comparison of calculated values of α_0 and α_2 [in kHz/(kV/cm²)].

Level	α_0	α_2	Reference
$2^2S_{1/2}$	40.7		This work
	40		[18]
	41.3		[19]
	42.07		[20]
	35.25		[21]
	36.42		[22]
	39.31		[23]
	42.37		[24]
	42.32		[25]
	41.87		[26]
$2^2P_{1/2}$	29.8		This work
	24		[18]
$2^2P_{3/2}$	29.8	0.55	This work
	24	1.8	[18]
	40	-10	[15]

where $W(n'L_J)$ is the energy of the level $n'L_J$.

The reduced matrix elements $|\langle nL || p || n'L' \rangle|^2$ are proportional to the line strength $S(nSL; n'S'L')$ of the multiplet

$$S(nSL; n'S'L') = (2S+1) |\langle nL || p || n'L' \rangle|^2. \quad (12)$$

Because the values given in Ref. [15] show large deviations from the experimental results, we have recalculated α_0 and α_2 by means of an analog formalism. Level energies and line strengths up to $n=5$ were taken from the tables of Moore [16] and Wiese, Smith, and Glennon [17]. Higher-level energies were calculated using a Coulomb approximation. The results of our calculations and a comparison with results of other authors are given in Table III.

VII. COMPARISON WITH THE SODIUM ATOM

There are two main differences between the behavior of the sodium and the lithium resonance lines in high electric fields. (i) The sign of the shift is different. The resonance lines of lithium are shifted to higher frequencies ($\alpha_0 < 0$), whereas the sodium D lines are shifted to lower frequencies ($\alpha_0 > 0$). (ii) The shift is about five times smaller for lithium than for sodium.

These observations can be easily understood if the positions of the levels $2^2S_{1/2}$, $3^2S_{1/2}$, $2^2P_{1/2,3/2}$, $3^2P_{1/2,3/2}$, and $3^2D_{3/2,5/2}$ in the Grotrian diagram are considered as shown in Fig. 5 (the main quantum numbers, except of the D levels, are higher by 1 for sodium).

As can be learned from former measurements [1,8] the shift of Na 3^2P to lower energies is about twice as large as the shift of the ground level, 3^2S . Therefore, a relatively large redshift of the line is observed. The most influencing levels relative to 3^2P are 3^2S , 4^2S , and 3^2D . In electric fields, the levels push each other and try to increase their energy distance. The strength of this interaction is proportional to the square of the dipole matrix element and inversely proportional to the energy difference of the levels. As can be seen in Fig. 5(b), the level 3^2P is much closer to 4^2S and 3^2D than to 3^2S and is therefore strongly pushed downwards and only slightly pushed upwards by 3^2S . Additionally, 3^2D lies close below 4^2P

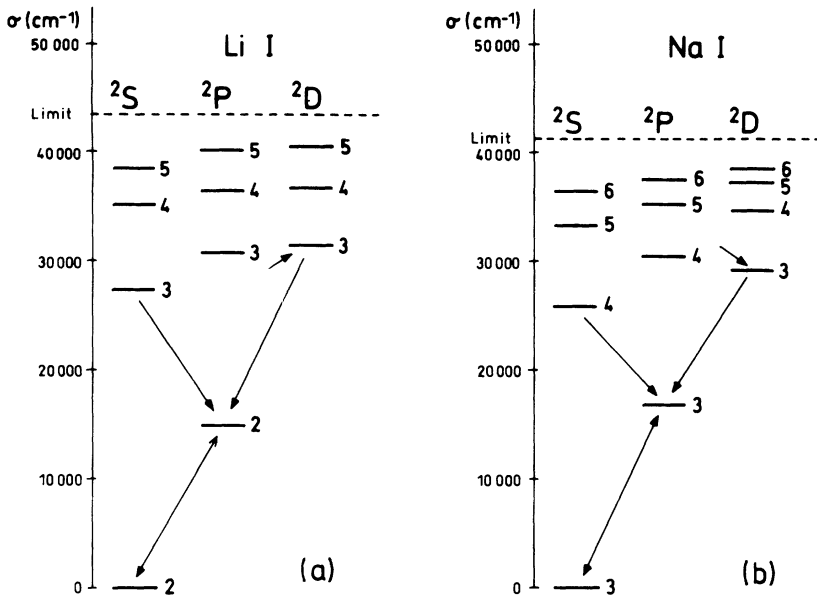


FIG. 5. Parts of the Grotrian diagrams of (a) Li and (b) Na showing the positions of relevant fine-structure levels for the D lines and the most important interactions concerning Stark-effect shifts (indicated by arrows) between the levels.

and is itself pushed strongly downwards. On the other hand, the ground level 3^2S is pushed downwards only by the interaction with 3^2P . So we have a strong shift of 3^2P and a smaller shift of 3^2S , both to lower energies. The difference in the shifts appears in the shift of the D lines, which are shifted to lower frequencies (towards the red).

In the case of Li the most influencing levels relative to 2^2P are 2^2S , 3^2S , and 3^2D . The level is about midway between 2^2S and 3^2S . Additionally, 3^2D lies above 3^2P and is pushed by this level to higher energy. In sum, 2^2P is pushed downwards by 3^2S and 3^2D but is pushed upwards by 2^2S , while 2^2S is pushed downwards mainly by 2^2P . The shift of 2^2S to lower energies is larger in this case as the shift of 2^2P to lower energies, and the energy

difference of the levels increases with increasing electric-field strength, appearing as a small blueshift of the D lines.

The sign of the tensor polarizability of the D_2 line is the same for Na and Li. Neglecting the hyperfine structure, $2^2P_{3/2}$ splits in two components $|M_J| = \frac{3}{2}$ and $|M_J| = \frac{1}{2}$; $2^2S_{1/2}$ has only $|M_J| = \frac{1}{2}$. So the excitation of $2^2P_{3/2}$ using π -polarized laser light ($\Delta M_J = 0$) must populate $|M_J| = \frac{1}{2}$. As can be seen from Figs. 3(c) and 3(d) the one component obtained with π -polarized laser light shows the larger shift. From this observation we know the quantum numbers $|M_J|$ of the components. Using Eq. (4) and $\Delta v_{\text{fine}} = \Delta v_i(\text{upper level}) - \Delta v_k(\text{lower level})$, one can easily deduce $\alpha_{2,i} > 0$.

- [1] L. Windholz and M. Musso, *Phys. Rev. A* **39**, 2472 (1989).
- [2] J. E. Blamont, *Ann. Phys. (Paris)* **2**, 551 (1957).
- [3] B. Budick, S. Marcus, and R. Novick, *Phys. Rev.* **140**, A1041 (1965).
- [4] R. W. Molof, H. L. Schwartz, T. M. Miller, and B. Beder-son, *Phys. Rev. A* **10**, 1131 (1974).
- [5] M. Musso, G. Zerza, and L. Windholz, in *11th International Conference on Atomic Physics; Abstracts of Contributed Posters*, edited by C. Fabre and D. Delande (Ecole Normale Supérieure, Paris, 1988).
- [6] L. R. Hunter, D. Krause, Jr., D. L. Berkeland, and M. G. Boshier, *Phys. Rev. A* **44**, 6140 (1991).
- [7] L. Windholz and C. Neureiter, *J. Phys. E* **17**, 186 (1984).
- [8] L. Windholz and C. Neureiter, *Phys. Lett.* **109A**, 155 (1985).
- [9] C. Neureiter, R. H. Rinkleff, and L. Windholz, *J. Phys. B* **19**, 2227 (1986).
- [10] M. Musso, C. Neureiter, and L. Windholz, *Proc. SPIE* **701**, 509 (1987).
- [11] H. Jäger, M. Musso, C. Neureiter, and L. Windholz, *Opt. Eng.* **29**, 42 (1990).
- [12] L. Windholz, H. Jäger, M. Musso, and G. Zerza, *Z. Phys. D* **16**, 41 (1990).
- [13] J. R. P. Angel and P. G. H. Sandars, *Proc. Soc. London Ser. A* **305**, 125 (1968).
- [14] M. Musso, *Z. Phys. D* (to be published).
- [15] R. W. Schmieder, A. Lurio, and W. Happer, *Phys. Rev. A* **3**, 1209 (1971).
- [16] Ch. Moore, *Atomic Energy Levels*, Natl. Bur. Stand. (U.S.) Circ. No. 467 (U.S. GPO, Washington, D.C., 1949), Vol. I.
- [17] W. L. Wiese, M. W. Smith, and B. M. Glennon, *Atomic Transition Probabilities*, Natl. Bur. Stand. Ref. Data Ser., Natl. Bur. Stand. (U.S.) Circ. No. 4 (U.S. GPO, Washington, D.C., 1966), Vol. I.
- [18] K. Murakawa and M. Yamamoto, *J. Phys. Soc. Jpn.* **20**, 1057 (1965).
- [19] S. A. Adelman and A. Szabo, *Phys. Rev. Lett.* **28**, 1427 (1972).
- [20] G. Maroulis and D. M. Bishop, *J. Phys. B* **19**, 369 (1986).
- [21] W. P. Langhoff and R. P. Hurst, *Phys. Rev.* **139**, A1415 (1965).
- [22] W. P. Langhoff, M. Karplus, and R. P. Hurst, *J. Chem.*

- Phys. **44**, 505 (1966).
- [23] G. W. F. Drake and H. D. Cohen, J. Chem. Phys. **48**, 1168 (1968).
- [24] H. J. Werner and W. Meyer, Phys. Rev. A **13**, 13 (1976).
- [25] T. Voegel, J. Hinze, and F. Tobin, J. Chem. Phys. **79**, 1107 (1979).
- [26] F. Maeder and W. Kutzelnigg, Chem. Phys. **42**, 95 (1979).
- [27] B. K. Rao and T. P. Das, Pramana **19**, 289 (1982).
- [28] G. Figari, G. F. Musso, and V. Magnasco, Mol. Phys. **50**, 1173 (1983).
- [29] C. Pouchan and D. M. Bishop, Phys. Rev. A **29**, 1 (1984).